J. Fluid Mech. (1996), vol. 327, pp. 139–160

On the motion of laminar wing wakes in a stratified fluid

By PHILIPPE R. SPALART

Boeing Commercial Airplane Group, PO Box 3707, Seattle, WA 98124-2207, USA

(Received 14 August 1995 and in revised form 10 June 1996)

We present numerical solutions for two-dimensional laminar symmetric vortex systems descending in a stably stratified fluid, within the Boussinesq approximation. Three types of flows are considered: (I) tight vortices; (II) those deriving from an elliptical wing lift distribution; and (III) those deriving from a 'high-lift' distribution, with a part-span flap on the wing. The non-dimensional stratification ranges from zero to moderate, as it does for airliners. For Types I and II, with high Reynolds numbers and weak stratification, the solutions confirm the theory of Scorer & Davenport (1970) (their article lacks a crucial link which we provide, equivalent to one of Crow (1974)). Contrary to common conceptions and observations in small-scale experiments, the descent velocity increases exponentially with time, as the distance between vortices decreases and the circulation of the vortices proper is conserved. With moderate stratification, wakes with sufficient energy also attain the accelerating régime, until the vortex cores make contact. However, they first experience a rebound, which is both of practical importance and out of reach of simple formulas. Type III wakes produce two durable vortex pairs which tumble, and mitigate the buoyancy effect by exchanging fluid with the surroundings. These phenomena are obscured by low wing aspect ratios, Reynolds numbers below about 10^5, or appreciable surrounding turbulence; this may explain why neither a clear rebound nor an acceleration can be reconciled with experiments to date. We argue that airliner wakes have very little inherent diffusion, and that a rapid end to the wake's descent must reveal effects other than simple buoyancy. In particular, stratification promotes the Crow instability.

1. Introduction

1.1. *Background*

In her 1975 review Widnall described a state of extreme disagreement regarding the interaction of airplane wakes and stratified atmospheres. Although the theoretical models were all two-dimensional and essentially inviscid, some predicted a faster descent while others predicted an end to the descent, if not an oscillation. The implications for Air Traffic Control (ATC) are obvious, since ATC relies on the wake sinking below the flight path. Experiments were also conflicting, although not as strongly, and conclusive numerical solutions absent. Literature since 1975 has generally supported the attractive and now widespread idea that the descent would end, roughly, after 1/4 of the Brunt–Väisälä period (Hill 1975; Tomassian 1979; Hecht, Bilanin & Hirsh 1981; Sarpkaya 1983; Greene 1986; Robins & Delisi 1990). However we do not perceive the wing aspect ratios, effective Reynolds numbers, and durations in these studies to be representative enough of airliners. Both laboratory

experiments and flight tests are beset by failures of the visualization techniques, which may not be faithful to the vorticity. Furthermore, no rational theoretical resolution has been published. Many destruction mechanisms compete in the experiment, and uncertainty can reign as to which mechanism, or combination, is the controlling one (Tomassian 1979; Sarpkaya 1983). With aspect ratios as low as 2 the kinetic energy of the cross-flow field (normalized with the circulation) is lower than for airliner wings; the left and right vortical regions touch. The high-Reynolds-number, high-aspect-ratio régime deserved a modern and determined numerical study.

As an example, in Hill's (1975) numerical solutions the descent was impeded, and arrested in many cases. He concluded somewhat in favour of Saffman's (1972) approximation, which predicts an oscillation, over those of Scorer & Davenport (1970) (hereafter SD) and Crow (1974), which predict an exponential acceleration. However, he obtained most of his evidence with fairly strong stratification, which Crow stated is out of the range of his theory (SD did not). The other theories also use small-perturbation arguments; therefore they are also weak-stratification approximations. We believe that, had he identified this issue and continued his runs (which the stability of a point-vortex method may not allow, not to mention 1974 computers), Hill would in fact have concluded in favour of SD and Crow for weak stratification; see in particular the case $\beta = 10^{-5}\mathrm{m}^{-1}$ in his figure 5.

In another example, Hecht *et al.* (1981) conducted the numerical simulation of a flight test. They discontinued the simulation when the wake levelled off, even before the test report ended. The real wake ('Run 8') was not destroyed then, and it is even stated that it exhibited Crow linking out of view of the camera. Not surprisingly, Hecht *et al.* (1981) found that at the end of their simulation 'the circulation remains high and the pair cannot be assumed to have dissipated'. A continuation of their simulation could well show the descent resuming, as in our results. Computational cost was a factor. We also note for future reference that, even though they used a turbulence model, their layer of buoyancy-generated vorticity was not noticeably thicker than ours and was almost all detrained from the oval region (see §3.2). They also found significant effects of the turbulence macroscale, thus underscoring the unavoidability of arbitrary parameters when a turbulence model is involved. This motivates our first fully exploring the laminar case.

1.2. *Major options of the study*

Our solutions are two-dimensional and have low viscous diffusion (2DLD, from here on), as we are interested in pure buoyancy effects in the wake far enough downstream for the slender-vortex approximation to be valid, and axial-flow effects to be negligible. There is evidence that the axial flow residual from Bernoulli effects and viscous momentum losses decays faster than the azimuthal flow. Strong axial flow is often seen again later, attributed to low core pressures, and leading to burst-like phenomena; we leave these for future work, necessarily three-dimensional.

Several experts in the field, including a referee of this paper, disqualify 2DLD results as they believe that strong turbulent mixing controls real airplane wakes. The turbulence, possibly seeded by that in the wing boundary layers, would fill the oval region of fluid that translates with the wake and destroy or disperse much of the initial circulation within the durations of interest, say two minutes for a medium-size airliner (Greene 1986). In contrast, in 2DLD simulations circulation is conserved very closely, and the vortical regions are far from filling the oval. We believe vortex rings fit the fully-turbulent description much better than wing wakes do, both because of additional sources of instability and because their generation process spreads even the

initial vorticity over a larger region. The two-dimensional version of the vortex-ring generator has been used (Liu & Srnsky 1990) but even with special care to control the stopping vortex (which is of opposite sense), it is not clear to us that the vortex system it creates is correct in terms of initial core size (Liu & Srnsky indeed report a rather different response to stratification). Inferences from rings to trailing vortices demand caution.

Even the impact of turbulence on single vortices is controversial, with evidence that turbulent mixing is greatly over-estimated by turbulence models developed for thin shear layers (Govindaraju & Saffman 1971; Zeman 1995). In their experiment on a single vortex without axial flow, Phillips & Graham (1984) find 'no discernible downstream change in the velocity field' and report rather erratic Reynolds-stress measurements, suggesting that a well-developed turbulent state has not evolved (the core has experienced over 4 full revolutions, which is a respectable 'non-dimensional age'). Devenport *et al.* (1996) for their wing-tip vortex also report 'little change in core parameters' over 30 chords streamwise (about 40 revolutions at the velocity peak), and 'at a rate that is not inconsistent with laminar diffusion'. They show how vortex meandering produces a spurious diffusion of the vorticity (although not circulation decay) in raw time-averaged measurements. It is also agreed that airliner wakes can remain vigorous for several minutes (Greene 1986, Conclusion 2), although they often do not. Condensation or smoke visualization show the 'apparent wake' (the marked region) remaining smooth and tight sometimes for several minutes, sometimes for a much shorter time. This would *not* happen if turbulence *inherent* to the wake were controlling, because such inherent turbulence would be reproducible (like boundary-layer turbulence). Our position is that the demise of the wake is much better described as a *self-destruction seeded by irreproducible external disturbances* (atmospheric or airplane-induced) than as a *reproducible gradual decay due to inherent turbulence*. When the external disturbances are weak enough, the self-destruction is delayed enough for 2DLD behaviour to closely approximate that behind airliners. We assert that 2DLD results, although not universal, are relevant. From an ATC point of view they can be considered as worst-case situations, and therefore may in fact be the most relevant. The reader should keep this 'diffusion controversy' in mind for the rest of the paper.

In this and related studies, we found that the initial core size, or equivalently the initial kinetic energy, and the shape of the wing lift distribution are both meaningful parameters. Therefore, using values representative of actual airplanes is necessary, while cases with tight vortices facilitate the validation of the theories. This motivates our three flow types. Our goals are to close the theoretical controversy that surrounds (2DLD) buoyancy effects, and to provide sound input for ATC considerations. This input is in no sense a complete answer, as we predict that in real life stratification and other influences collaborate and compete in many non-trivial manners.

2. Governing equations and numerical method

2.1. *Equations, boundary and initial conditions*

We use the Boussinesq approximation, as did most workers in the field. The typical amount of descent of an airliner wake is up to about 250 m, while the length scale L of the density gradient is typically 10^4 m; therefore, density variations of only a few percent take place. Besides the two-dimensional incompressible Navier–Stokes equations for the velocity vector $\boldsymbol{U}$ and kinematic pressure p we solve for a non-

dimensional density perturbation field ρ. The density in the inertial term of the momentum equation is set to 1. The equations are

$$\nabla \cdot \boldsymbol{U} = 0, \tag{1a}$$

$$\boldsymbol{U}_t + \boldsymbol{U} \cdot \nabla \boldsymbol{U} = -\nabla p + \nu \nabla^2 \boldsymbol{U} + \rho \boldsymbol{g}, \tag{1b}$$

$$\rho_t + \boldsymbol{U} \cdot \nabla \rho = \frac{\nu}{Pr} \nabla^2 \rho. \tag{1c}$$

Here, ν is the kinematic viscosity and the Prandtl number Pr is set to 0.71.

In the lateral direction, x, periodic conditions are used for all variables, and the period is denoted by λ_x. The flow is also symmetric with respect to $x = 0$. In the vertical direction, y, periodic conditions are used for the variations with respect to a background gradient. The gravity vector $\boldsymbol{g}$ is pointing in the negative y-direction. The mean gradient $\partial \rho / \partial y$ is denoted by $-1/L$ and the Brunt–Väisälä frequency is $N \equiv (g/L)^{1/2}$. There is also a background pressure gradient, adjusted so that it would maintain hydrostatic equilibrium (i.e. stationary mean v) with the *initial* density field.

Periodic conditions allow a Fourier-based spectral numerical method (Gottlieb & Orszag 1977), known for its high accuracy and moderate cost, exact volume conservation (1a), and absence of numerical dissipation. Periodicity makes budgeting of the impulse and kinetic and potential energy straightforward. On the other hand, differences between the periodic solution and the true infinite-domain solution must be assessed. Usually λ_x is smaller, so that lateral periodicity effects exceed the vertical effects.

The effect of the periodicity on the mean vertical velocity is corrected by setting the average v-component in the periodic box to $-\pi I_0/(6\lambda_x^2)$ in the initial condition, where I_0 is the initial impulse (defined shortly). This correction, derived by comparing the periodic and the infinite-domain Biot-Savart kernels (Lamb 1932; Art. 156), is indispensable as it may be as high as 20% of the initial descent velocity. The initial descent velocity in the figures and in additional tests of our code is in excellent agreement with the infinite-domain value. The effect of periodicity on the strain tensor is not corrected, but is of higher order in λ_x: the ratio of parasitic to correct strain rate at the vortex centre is $(\pi b/\lambda_x)^4/15$ where b is the distance between the two vortices. As a result, a value $\lambda_x = 4b$ is sufficient. The vertical period is chosen so that during the simulation the pair travels by a distance less than λ_y, with a margin at least equal to λ_x.

The initial conditions are as follows. The scalar is undisturbed: $\mathrm{d}\rho/\mathrm{d}y = -1/L$. The mean u-component is zero by symmetry, and the mean v has been discussed. A smooth vorticity distribution ω, resolvable by the grid, is created by the convolution of a Gaussian G with an 'ideal' singular distribution $\tilde{\omega}$. This ideal distribution derives from the circulation distribution $\Gamma(x)$ on a planar wing located at $y = 0$:

$$\omega = \tilde{\omega} * G; \qquad \tilde{\omega} = -\frac{\mathrm{d}\Gamma}{\mathrm{d}x}\,\delta(y); \qquad G(x,y) \equiv \frac{1}{\pi\sigma^2}\,\exp\left(-\frac{x^2+y^2}{\sigma^2}\right). \tag{2}$$

Here δ is the Dirac distribution.

The circulation distributions of Type I, II, and III are shown in figure 1. They are symmetric ($\Gamma(-x) = \Gamma(x)$) and normalized to have the same 'root circulation' $\Gamma(0) = \Gamma_0$ and initial impulse $I_0 \equiv \int \Gamma \,\mathrm{d}x \equiv \Gamma_0 b_0$. This defines the 'effective span' b_0. These three wakes would be indistinguishable to the simple wake models. For Type I the ideal circulation is a step function:

$$\Gamma(x) = \begin{cases} \Gamma_0 & \text{if } |x| < b_0/2 \\ 0 & \text{if } |x| > b_0/2, \end{cases} \tag{3}$$

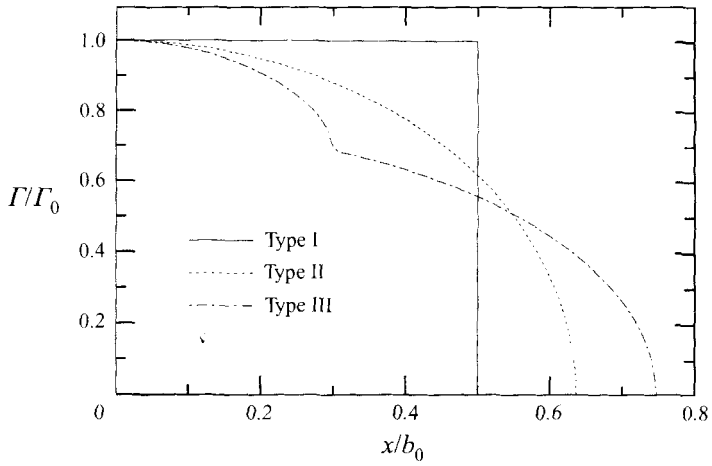

FIGURE 1. Distributions of circulation.

so that the initial vorticity ω is made of two circular Gaussian vortices with core size σ, as in Robins & Delisi (1990). For small σ/b_0, without stratification, this initial condition gives a quasi-steady flow.

For Type II the ideal circulation is elliptical:

$$\Gamma(x) = \begin{cases} \Gamma_0(1 - 4x^2/b_w^2)^{1/2} & \text{if } |x| < b_w/2 \\ 0 & \text{if } |x| > b_w/2, \end{cases} \tag{4}$$

where $b_w = 4b_0/\pi$. This flow starts with a transient, the 'initial roll-up', which leads to a quasi-steady flow if unstratified.

For Type III a distribution generic of some airliners in high-lift condition was defined by assembling two elliptical distributions such as the one for Type II. The step in Γ at $x = 0.3b_0$ is attributed to an inboard flap, partially offset by the opposite lift on the horizontal tail. The kinetic energy of the (u, v) field in an infinite domain is about 0.31, normalized with Γ_0 (as opposed to 0.39 for Type II), and the lifting-line 'efficiency factor' is $e \approx 0.93$. The motivation is that we have found that the mature wake of Type III contains two vortices on each side. This is true in low-diffusion simulations, as well as in a wind tunnel up to 13 spans behind a generic high-lift model with a circulation Reynolds number of about 900 000 (de Bruin *et al.* 1996 and unpublished further work by the same group, 1996). The resulting flow is quasi-periodic in time even after initial roll-up and, unlike the quasi-steady wakes from Types I and II, this wake is not followed from the initial altitude by a 'bubble' of fluid. We anticipated that the sustained exchange of fluid with the surroundings would weaken the buoyancy effect.

Besides the Type, I to III, the problem we defined has three non-dimensional parameters: the normalized width of the initial vorticity, $r_c \equiv \sigma/b_0$; the Reynolds number $Re \equiv \Gamma_0/\nu$; and the 'stratification number' (inverse Froude number) $N_0^* \equiv 2\pi N b_0^2/\Gamma_0$. The spread of the vorticity is controlled by r_c and Re which are set low and high enough, respectively, to not influence the conclusions. In the figures, lengths and times are normalized using $\Gamma_0/2\pi$ and b_0, and simply denoted by x, t, and so on. Circulations are still normalized with Γ_0 itself.

2.2. *Numerical method*

Fourier series are used as spatial discretization, with the nonlinear terms calculated in real space (Gottlieb & Orszag 1977) and de-aliasing applied with the 2/3 rule. Tests without de-aliasing resulted in sudden instabilities, which shorter time steps did not suppress. Other authors have reported stability problems for the stratified equations, which we attribute to the extra derivative present in the coupled system (1). The de-aliased code has been fully reliable with automatic time-step adjustments to hold the peak CFL number.

Since the differentiations of the stream function, pressure, and Laplacian are performed exactly in Fourier space, it is immaterial whether the method is presented using primitive variables, stream function, or vorticity. The only decision was which form of the nonlinear terms to carry from real to Fourier space; we chose ($v\omega$, $-u\omega$, $u\rho$, $v\rho$) for reasons of convenience. The time integration uses the low-storage semi-implicit Runge–Kutta-based scheme of Spalart, Moser, & Rogers (1991), and the peak CFL number is usually set to 2. This time-integration scheme is not energy-conserving (in contrast with the spatial discretization), but energy budgets show the 'numerical' energy loss to be much smaller than the viscous loss calculated from the integrals of the enstrophy and density gradient squared, even at a Reynolds number of 10^5. Numerical oscillations are also monitored to detect possible insufficient resolution.

A typical numerical resolution is as follows. In the x-direction, 400 points cover the period $\lambda_x = 4b_0$ (shortest resolved wavelength: $0.03b_0$). The resolution is the same in y: $\lambda_y = 30b_0$ and 3000 points. The viscosity is $\nu = 2.5 \times 10^{-5}\Gamma_0$ ($Re = 40\,000$). Unstratified simulations can be run at any Reynolds number without catastrophic inaccuracies, provided the initial condition is well resolved, as the exact vorticity is known to remain bounded in two dimensions and the numerical method duplicates this rather well. It is the resolution of the density that sets the Reynolds-number range that can be accommodated accurately. The strain rate S at the stagnation points is $\sqrt{3}\Gamma_0/(2\pi b_0^2)$, which creates internal density boundary layers that approach error functions with length scale $\sigma' = (2\nu/SPr)^{1/2} = 0.016b_0$. With a grid spacing $\Delta x = 0.01b_0$ the spectral method is able to resolve these gradients with a very small amount of 'ringing'. For other cases the grid spacing follows the power $-1/2$ of the Reynolds number. For a case with moderately thin cores the time step is initially about $6 \times 10^{-3} b_0^2/\Gamma_0$, and the simulation uses about 15 000 steps.

In the calculations of Robins & Delisi (1990) a damping term dependent on the x-wavenumber was used; the shortest wavelength unaffected by damping was about $b_0/2$, so that our estimate of the effective Reynolds number Γ_0/ν_{eff} is only about 250. Their high value $r_c = 0.2$ was not conducive to the appearance of the finer structures. This motivates our earlier remarks on effective Reynolds numbers, and is not disputed by the authors; our study has been vastly more costly than theirs.

3. Structure and scaling of the asymptotic state

3.1. *Overview*

We consider a state as described by SD, Saffman (1972), Crow (1974), and others, which we believe is the only one amenable to a simple theory. The flow is mature, quasi-steady, and nearly inviscid. The vorticity created initially, positive in the right-hand wake half, has remained tight and is segregated from the (predominantly negative) vorticity created by buoyancy. The vortex spacing b, suitably defined, may deviate from b_0. A tadpole-shaped region of light fluid of size proportional to b

is propelled downward by the vortices, leaving a narrow tail of light fluid. The buoyancy-generated vorticity is confined to a thin layer on the light–heavy interface.

We use Type-I numerical solutions to guide the theoretical effort. By combining the initial core size and the subsequent viscous diffusion we find that the vorticity segregation requires the condition $\sigma^2 + 4\nu t \ll b^2$. The second requirement of a tractable model is for the density to be close to uniform over the neighbourhood of the vortices. The density anomaly $\Delta\rho$ with the outside is $-Y/L$ where Y denotes the position of the vortices relative to the initial state. We therefore require $b \ll |Y|$; the wake descent has been much larger than its (current) size, although still much smaller than the length scale L of the density gradient for the Boussinesq approximation to apply. We require a small perturbation relative to the neutral state, therefore the current stratification number $N^* \equiv 2\pi N b^2/\Gamma$ must be small. It does not follow that the initial stratification number N_0^* was small, because b can decrease significantly, as we show below.

The two asymptotic conditions become

$$\sigma^2 + 4\nu t \ll b^2 \ll \left[\frac{t\Gamma}{b}\right]^2. \tag{5}$$

They require tight initial cores, $\sigma \ll b$. The time needs to be large compared with b^2/Γ, but small compared with b^2/ν, hence the need for a large Reynolds number, $Re \gg 1$.

3.2. *Flow pattern and the detrainment issue*

In figure 2 we present a weakly stratified case, and a neutral case ($g = 0$) for reference. Fair estimates of the inequalities needed, as opposed to the asymptotic requirements (5), are $25(\sigma^2 + 4\Gamma t/Re) \leqslant b^2$ and $|Y| \geqslant 20b$. These are reached with the parameters (*Re*, and so on) used here. The uniformity of density is well indicated, and the proportions of the light-fluid region are those of the oval of fluid that follows a vortex pair. The unstratified wake descent is within 1% of the descent of a point-vortex pair in an infinite domain.

In the stratified case the vorticity segregation is clear; the buoyancy-generated vorticity is overwhelmingly detrained, instead of circulating around the vortices (refer to Widnall's 1975 figure 2). If that is so, we arrive at a clear scaling by considering the flow as quasi-steady in a reference frame that follows the vortices, and accounting for the separate contributions to the near-equilibrium. In contrast, past workers without the benefit of low-diffusion numerical solutions made widely diverging assumptions at this juncture.

We introduce the notation ω_1 for the vorticity created initially (positive, found near (0.4, –16.6) in figure 2*c*) and ω_2 for that generated by buoyancy and present near the vortices (negative, found near (0.7,–16.6)), with the corresponding notation $\boldsymbol{U}_1$ (meaning $\nabla \times \boldsymbol{U}_1 = \omega_1$) and $\boldsymbol{U}_2$, as well as Γ_1 and Γ_2. The vorticity contained in the tail is ω_3 (negative, found near (0.1,–15.6)). The exact boundary between ω_2 and ω_3 does not matter ($y = -15.7$ would be plausible); its offset relative to the vortex just needs to be proportional to b. For the figures we explicitly define $b/2$ and Y as the coordinates of the peak positive ω value (0.34 and –16.64 in figure 2*c*).

We assume $\Gamma_2 \ll \Gamma_1$, as supported by integrals of the field in figure 2(*c*) and verified later. Because the vortex is surrounded by irrotational fluid, its circulation is stationary: $\mathrm{d}\Gamma_1/\mathrm{d}t = 0$, and is intact to leading order: $\Gamma_1 = \Gamma_0$. The velocities are dominated by ω_1 and therefore of order Γ_1/b. The evolution of ω_2 results from a balance between buoyancy and convection by $\boldsymbol{U}_1$. Buoyancy forces (the term $g\partial\rho/\partial x$ in the curl of (1*b*)) are proportional to $g\Delta\rho$, itself equal to $N^2 Y$, so that their contribution

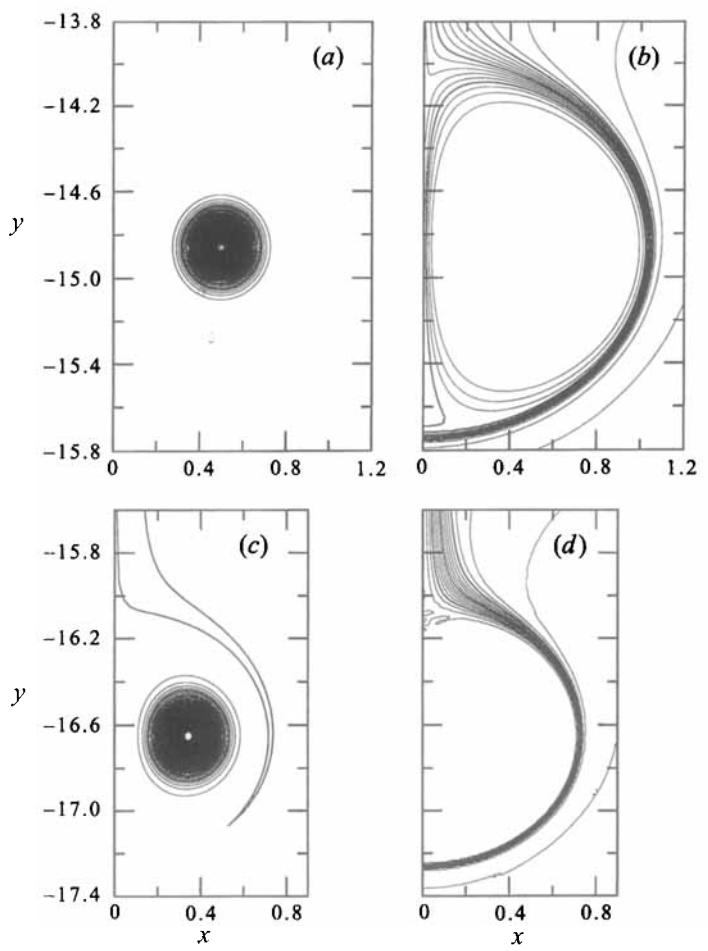

FIGURE 2. Distributions of (a, c) vorticity and (b, d) density in solutions of Type I, with $Re = 4 \times 10^4$, $r_c = 0.05$, and $t = 15$. (a, b), $N_0^* = 0$; (c, d) $N_0^* = 0.1$. Right half-plane only.

to $\mathrm{d}\Gamma_2/\mathrm{d}t$ is proportional to $N^2 Y b$. The effect of convection by $\boldsymbol{U}_1$ (the term $\boldsymbol{U}_1 \cdot \nabla \omega_2$ in the curl of (1b)) on $\mathrm{d}\Gamma_2/\mathrm{d}t$ is proportional to $\Gamma_2 \Gamma_1 / b^2$. These two terms dominate the evolution of ω_2, therefore we have to leading order

$$\Gamma_2 = C_1 \frac{b^3 N^2 Y}{\Gamma_1} \tag{6}$$

for some positive constant C_1. Also to leading order, the descent velocity is

$$\frac{\mathrm{d}Y}{\mathrm{d}t} = -\frac{\Gamma_1}{2\pi b}. \tag{7}$$

Finally we note that ω_2 is stronger above the vortex than below as a result of the build-up of vorticity along the streamline, thus inducing a velocity that contracts the vortex pair. To leading order,

$$\frac{\mathrm{d}b}{\mathrm{d}t} = C_2 \frac{\Gamma_2}{b} \tag{8}$$

for some positive constant C_2.

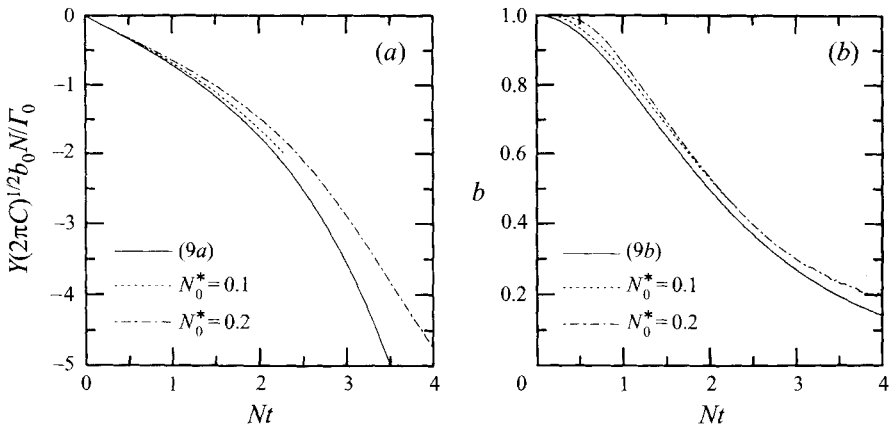

FIGURE 3. (*a*) Descent and (*b*) spacing of Type-I vortices, theory (9) and simulations. $r_c = 0.05$, $Re = 4\ 10^4$.

We denote $C_1 \times C_2$ by C, and solve three equations for three unknowns:

$$Y = -\frac{\Gamma_0}{(2\pi C)^{1/2}Nb_0}\sinh\left((C/2\pi)^{1/2}Nt\right), \tag{9a}$$

$$b = \frac{b_0}{\cosh\left((C/2\pi)^{1/2}Nt\right)}. \tag{9b}$$

According to (6), (9) Γ_2 decays to zero for large times at the rate $\exp(-(2C/\pi)^{1/2}Nt)$, consistent with our earlier assumption $\Gamma_2 \ll \Gamma_1$. SD also made the point that Γ_2 peaks (at a time of about $Nt = 1$, with a value of about $0.15\Gamma_0 N_0^*$) and then decays. The instantaneous stratification number $N^* \equiv 2\pi N b^2/\Gamma_1$ decreases to zero.

Figure 3 shows a validation of (9), using weakly stratified Type-I cases and $C = 2.75$. It illustrates both the initial transient, during which (6) has not been established and which introduces a slight time shift relative to (9), and faintly the eventual saturation when the viscous spreading of the core and the contraction together defeat the model (predictably, viscous cancellation pushes the vorticity peaks apart and reduces the velocity). The improved agreement as N_0^* decreases is also clear. Direct tests of (6), (8) using these solutions, not shown, are satisfactory and strongly suggest that C is in the bracket [2.6, 2.9] ($C_1 \approx 10$, $C_2 \approx 0.275$ with a plausible border between ω_2 and ω_3). Another feature of the model confirmed by the numerical results is the conservation of Γ_1 (with ω_1 extracted as the vorticity of positive sign found in the head region). The budgeting of the global circulation $\Gamma_1 + \Gamma_2 + \Gamma_3$, of the impulse (see (10) below), and kinetic and potential energy was made and found to be very satisfactory. This essentially rules out coding errors and serious numerical errors.

3.3. *Scorer & Davenport's derivation and Saffman's criticism*

Our analysis so far is similar to that of SD and produces the same result (9), with one crucial difference. We present C as a universal constant, but one that results from a non-trivial solution for ω_2; in contrast they directly give the value $C \approx 2.85$, which falls within our calculated bracket. This must be explained, especially in view of Saffman's (1972) sharp criticism of the SD analysis. In an internal report he gave us, Crow (1974) correctly arrives at $C \approx 2.85$, by an argument that is superficially

different from ours, and he defends SD. Crow also gives a convincing if very brief argument to justify full detrainment of ω_2 (his p. 6).

We concur with Saffman that the SD presentation is deficient; it could even be fortuitously correct. On p. 457 they identify the rate of change of impulse due to the effect of buoyancy on the head region (the product of the area of that region and the anomaly $g\Delta\rho$), and immediately equate it to $\Gamma_0 \mathrm{d}b/\mathrm{d}t$, in our notation. This does not follow, because the buoyancy acts only to create vorticity on the interface. It does not displace the primary vortices; in fact the vorticity source term is zero near the vortices, since ρ is assumed uniform (figure 2*d*). SD inherited this 'leap' from Turner (1960). The deficiency is resolved by the following argument.

Let us for now ignore the 'tail' ω_3 of the vorticity distribution. A theorem states that in the absence of buoyancy forces a system of vorticity conserves its impulse, $I \equiv \int\int x\ \omega\ \mathrm{d}x\mathrm{d}y$. An equation for $\mathrm{d}I/\mathrm{d}t$ is readily derived from (1). The pressure term clearly does not contribute to $\mathrm{d}I/\mathrm{d}t$, and it is found that the viscous term does not either. The remaining terms are convection and buoyancy, which can be rearranged as follows:

$$\frac{\mathrm{d}I}{\mathrm{d}t} = \iint u\ \omega\ \mathrm{d}x\mathrm{d}y + g \iint (\rho - \rho_\infty)\ \mathrm{d}x\mathrm{d}y \tag{10}$$

where $\rho_\infty(y)$ is the density as $x \to \pm\infty$. We verify that the first term on the right is zero, if u and ω match (meaning $\omega = \nabla \times \boldsymbol{U}$) and $\boldsymbol{U}$ is divergence-free, in accordance with the basic theorem. A consequence is the 'reciprocal' property that $\int\int u_1\omega_2\ \mathrm{d}x\mathrm{d}y = -\int\int u_2\omega_1\ \mathrm{d}x\mathrm{d}y$. The integral theorems are correct both for infinite domains and for periodic domains, provided only that $\omega = 0$ in a neighbourhood of the periodic boundary $x = \pm\lambda_x/2$ so that there is no viscous flux there and that $\rho_\infty(y)$ is re-defined as $\rho(\pm\lambda_x/2, y)$.

We now separate the impulse into I_1 and I_2, express all the identities and assumptions we have gathered, and arrive at the following equations:

$$\Gamma_0 \frac{\mathrm{d}b}{\mathrm{d}t} = \frac{\mathrm{d}I_1}{\mathrm{d}t} = \iint u_2\omega_1\ \mathrm{d}x\mathrm{d}y = -\iint u_1\omega_2\ \mathrm{d}x\mathrm{d}y = g\iint (\rho - \rho_\infty)\ \mathrm{d}x\mathrm{d}y - \frac{\mathrm{d}I_2}{\mathrm{d}t}. \tag{11}$$

Now in the fully-developed régime, according to (6), (9), $\mathrm{d}I_2/\mathrm{d}t \ll \mathrm{d}I_1/\mathrm{d}t$. We then arrive at an equation consistent with (6), (8), the same equation as SD:

$$\Gamma_0 \frac{\mathrm{d}b}{\mathrm{d}t} = g \iint (\rho - \rho_\infty)\ \mathrm{d}x\mathrm{d}y = Cb^2N^2Y \tag{12}$$

where Cb^2 is the area of the 'tadpole's head', now identified with the oval that follows the vortex pair in the ideal situation, $C \approx 2.85$. However, there is no indication that SD or Turner used the reasoning in (10)–(12) and in particular the reciprocal property. We did not obtain Davenport's thesis, on which the paper was based. For now we consider the success of the SD/Turner formula as dependent on an intuition of the reciprocal theorem, and on the neglect of $\mathrm{d}I_2/\mathrm{d}t$, neither of which they put into words.

Regarding Saffman's analysis, we cannot agree with his supposition on p. 112 that b is constant and Γ_1 varies. Again, there is no direct effect of buoyancy on ω_1. The result of this supposition is that the wake is predicted to oscillate, instead of speeding up exponentially. Of the studies quoted by Widnall (1975), only SD and Crow assumed full detrainment of the ω_2 vorticity. Therefore, we expect that none of the other ones would be consistent with our findings; some may well have addressed other régimes than the one here.

We are left with estimating the effect of the tail vorticity ω_3, which we have neglected until now. The velocity in the tail is low, and we can estimate its width from area conservation for the fluid region that was at $y \geqslant 0$ initially (the light-fluid region). The head travels at a velocity $\Gamma_0/(2\pi b)$ and its area decreases at a rate $(2C^3/\pi)^{1/2}Nb^2$ (use (6), (8)). Therefore the width of the tail near the head is $(8\pi C^3)^{1/2}Nb^3/\Gamma_0$ (this gives a width of 0.12, not inconsistent with figure 2*c*, *d*). It tends to zero as fast as $|Y|^{-3}$, much faster than b which is proportional to $|Y|^{-1}$. As a result the total impulse of the tail is finite as $t \to \infty$, so that the velocity it induces near the head tends to zero at least as fast as $|Y|^{-2}$, compared with the velocity U_1 which is proportional to $|Y|$. We conclude that in the fully developed régime the velocity induced by ω_3 can be neglected, and that the reasoning in (10)–(12) is valid. Figure 3 shows no sign that the length of the tail, which starts at zero, has much impact. The initial transient takes only a few units of t (each unit corresponds with one b_0 of descent), well explained by the requirement for ρ deviations within the oval to become small compared with $\Delta\rho$.

4. Behaviour for finite time, energy, and stratification

4.1. *Comparison with experimental results*

Sarpkaya (1983) studied the flow behind low-aspect-ratio delta and rectangular wings and stratification numbers $N_0^* = 1$, 3/4, 1/2, and 0. The results, confirmed by a calculation of Robins & Delisi (1990) with $r_c = 0.2$, support the idea that stable stratification arrests the wake descent, although Sarpkaya did not make such an explicit statement. He found no experimental support at all for the SD equations (9). In an attempt to reconcile our stand with Sarpkaya's results we conducted simulations with a moderate Reynolds number ($Re = 2 \times 10^4$, which falls within his range), and values of r_c intended to roughly duplicate the larger cores generated by the low-aspect-ratio wings. We settled on the value $r_c = 0.25$. The initial kinetic energy is 0.25, normalized by Γ_0^2, as opposed to about 0.39 for an elliptical distribution (Type II). The cores do not overlap appreciably at $t = 0$; therefore this initial condition is not excessively diffuse.

In figure 4 our results agree quite well with Sarpkaya's for as long as he presented his. We must mention that unstratified results, not shown, are not in as good an agreement (from $t \approx 2.5$ on there is a shift between his results and the ideal descent rate, which he attributed to differences between delta and rectangular wings). Note that we did not even invoke any enhanced 'turbulent viscosity' to obtain agreement. Thus, we consider his experimental results as explained, but not representative enough of airliner wakes, on the basis of aspect ratio, Reynolds number, and durations (he does not comment on why some curves terminate before $t = 3$ while most extend to $t = 6$, but we presume the wakes broke up). We view his conclusions as correct and firmly guard against an interpretation of his results to mean that as a rule, *under the effect of stratification alone*, wakes only descend to a finite height. He clearly stated that other decay mechanisms were at play, and we return to this in §5.2.

Tomassian's results (1979) first show an encouraging contraction of the pair but it is rapidly overwhelmed by an expansion, unrelated to stratification, which he concisely attributed to 'turbulence'. As we never observe such an expansion, we do not attempt a direct comparison. We do note that the spacing in stratified flow is as low as 2/3 of the spacing in unstratified flow, which is not at all inconsistent with the theory.

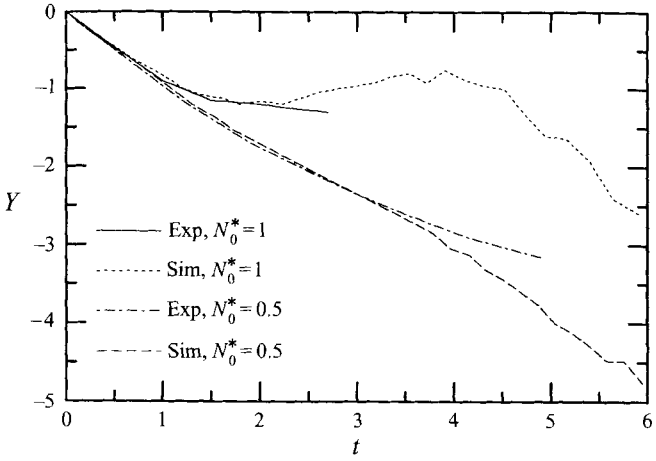

FIGURE 4. Propagation of Type-I flows with $r_c = 0.25$, $Re = 2 \times 10^4$, compared with experimental results of Sarpkaya, visually averaged.

4.2. *Unstratified Type-II solutions*

The solutions used in §3 were *designed* to lead to the asymptotic state, in particular by using tight vortex cores; while a mathematical question has been answered, the relevance to realistic wake vortex systems is not established. The simplest useful measure of realism may be the ratio of kinetic energy to Γ_0^2 (Spreiter & Sacks 1951). First we consider the Type-II, elliptical-wing flow, which is well-known and a fair approximation of 'clean-wing' configurations. An intriguing property, independent of stratification, seems worth a digression. Figure 5 is obtained from a flow of Type II, after the initial roll-up: $t = 1$. At that time and Reynolds number the vorticity contours are smooth and roughly axisymmetric (evidence is that the vorticity centroid is at $x = 0.500$, and the peak location wavers between 0.495 and 0.505). We considered the circulation $\tilde{\Gamma}(r)$ around circles of radius r centred at the vorticity peak (but clipped at $x = 0$ if $r > 0.5$). The apparent circulation deduced from a horizontal cut of the vertical velocity component, corrected for the field of the other vortex, gives noisier but consistent results; this is of interest because it is what some ground-based experimental systems measure in flight tests.

Our profiles of azimuthal velocity (defined as $u_\theta \equiv \tilde{\Gamma}/(2\pi r)$) in figure 5(*a*) match the experimental trend shown in Widnall's (1975) figure 1, namely, the velocity is lower than predicted by Spreiter & Sacks (1951) for moderate r, and much higher for small r. They lead to the same kinetic energy; recall that Spreiter & Sacks (1951) adjusted the core size to match the energy (we corrected the error in their equation (15), which increases the core size by 11%, see Milne-Thomson 1958). For small r_c the core radius, defined by the location of the peak tangential velocity, is very small. The disagreement with Spreiter–Sacks has been a puzzle from flight tests. The Spreiter–Sacks energy argument is no more successful when combined with a Gaussian vorticity core instead of a 'top-hat' core (not shown). An assumed distribution with a $\omega \propto r^{-2}$ range (equivalent to a logarithmic circulation, see below) appears necessary; unfortunately it needs to be 'clipped' both for small and for large radius, and at least three constraints are needed to complete such a model, as opposed to just one for Spreiter & Sacks (1951).

Figure 5(*b*) shows that the circulation behaves logarithmically for over a decade in r. The Spreiter–Sacks formula $\tilde{\Gamma} = \min(1, [r/0.109]^2)$ and the Hoffmann–Joubert (1963)

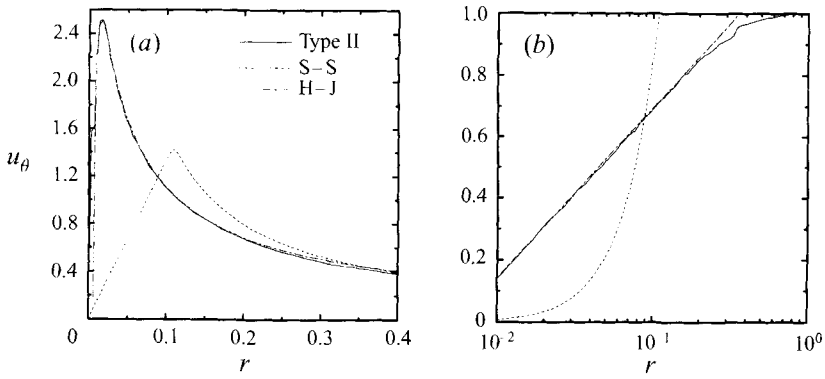

FIGURE 5. Azimuthal velocity and circulation at a radius r. Type-II flow, $Re = 10^5$, $r_c = 0.01$, $t = 1$; also Spreiter–Sacks and Hoffmann–Joubert models.

formula $\tilde{\Gamma} = 0.27(1 + 0.93\log(r/0.019))$ are also shown (the parameters $\Gamma_1 = 0.27$ and $r_1 = 0.019$ were adjusted to obtain a fit, while 0.93 comes from H–J). The logarithmic range increased towards $r = 0$ as r_c was reduced from 0.02 to 0.01, the outer part being unchanged. However, the log law extrapolates to $\tilde{\Gamma} = 0$ at $r \approx 0.007$, therefore this behaviour could not continue indefinitely as r_c is reduced further. The logarithmic behaviour appears too clearly indicated to be fortuitous, but we are not optimistic about a theory to explain it. The relationship between R and X, discussed by Widnall (1975) on p. 149 (defined by $\tilde{\Gamma}(R) = \Gamma(b_w - X)$), was plotted and found unremarkable. The logarithmic range extends roughly over $0.1 \leqslant \tilde{\Gamma} \leqslant 0.9$, that is, out of the range of the near-tip Taylor expansion of $\Gamma(x)$ (square root of the distance to the tip). Thus it should be out of reach of the analysis of Moore & Saffman (1973).

The logarithmic behaviour cannot be fully general; for instance we show below that some lift distributions produce two durably separate vortices per side, therefore even the near-axisymmetry after initial roll-up is not general. We calculated a flow with $\Gamma(x)$ the average of a Type-I and a Type-II flow; the circulation does display a logarithmic region, about half as long as for Type II (a factor of 4 in r, instead of 20) and with less slope ($r\mathrm{d}\tilde{\Gamma}/\mathrm{d}r \approx 0.15$, instead of 0.24). This suggests that a logarithmic region of some length can be expected from smooth lift distributions, but the slope is not universal if normalized with Γ_0. In the past the formula has often been used with r_1 the location of peak $\tilde{\Gamma}/r$. In that case the slope must be 1, not 0.93, and success is measured only in terms of the curvature of the function, not an easy proposition in view of experimental scatter.

The Hoffmann–Joubert logarithmic formula has received experimental support and seems very successful here, although very sensitive to the value of r_1: even setting it to 0.020 instead of 0.019 degrades the fit considerably. More importantly, our results suggest that a property of the inviscid roll-up has been erroneously attributed to turbulent mixing (our solution is two-dimensional, and therefore surely not turbulent). This would not come as a surprise, because in our opinion the 'turbulent' justifications provided by Hoffmann & Joubert (1963) are physically weak. Govindaraju & Saffman (1971) provide an alternative derivation, but 'fundamentally different' and implying the opposite sign for the shear stress. Other factors add confusion. Since Hoffmann & Joubert used two blades at opposite angles of attack in their experiment, there is no reason why their roll-up should be very close to that behind a wing. On the other hand, many of the subsequent measurements that

display the logarithmic behaviour (often more pronounced than in the original paper itself) did derive from wings. Our log layer is also much longer than the original (a factor of about 20 in r, as opposed to about 4).

We conclude that the $\widetilde{\Gamma}$ findings, although we are far from a theoretical closure, are useful both in terms of reconciling flight-test and numerical results, and in discarding the Spreiter–Sacks model, as well as any turbulent basis for the logarithmic dependence of the circulation. They are also damaging for the Betz approximation, which implies $\widetilde{\Gamma} \propto r^{1/2}$ (Widnall 1975); plots of $\widetilde{\Gamma}$ *vs.* $r^{1/2}$ (not shown) are unconvincing. At best, that approximation works only up to $\widetilde{\Gamma} \approx 0.1$, and was 'covered' by viscous effects.

4.3. *Stratified Type-II solutions*

We now consider longer, stratified Type-II solutions. With airliners in mind, the durations of interest are up to about $t = 15$, that is, the time needed for the wake to descend 15 effective spans at the ideal rate. Typical stratification numbers N_0^* are in the range of about 0.1 to 1.2, with 1.2 being extreme since it arises for an airplane larger than a Boeing 747 (N_0^* is roughly proportional to the square root of the weight) and strong stratification, $N \approx 0.03$ s^{-1}. Thus we differ with Crow's (1974) position that $N_0^* = 0.16$ is the upper limit of interest. The difference originates in his estimate of b_0 for a Boeing 747, which is quite low (with Γ_0 correspondingly high), and in his position that $N = 0.019$ s^{-1} is already 'untypically stable'. According to Charney & Drazin (1961), $N = 0.019$ s^{-1} is in fact typical at sea level in the winter. We cannot confine our study to the weakly stratified régime, $N_0^* \ll 1$. We choose values of 0.2 and 1; recall that the intensity of the stratification varies like N_0^{*2}. For the Reynolds number and sheet thickness, manageable values (in terms of computing cost) are $Re = 10^5$ and $r_c = 0.01$. Unlike Type-I flows, the Type-II velocity profile is independent of r_c except very near the centre. The $N_0^* = 1$ case was repeated with both numerical periods (λ_x and λ_y) doubled, causing only a 3% difference in the descent; this confirms the adequacy of the boundary conditions we used.

Figure 6 indicates that the Type-II cores are indeed thin enough for the acceleration mechanism to be relevant, not indefinitely, but for much of the duration of interest. Again our result for $N_0^* = 1$ is in agreement with the experiment of Sarpkaya (1983) and the calculations of Robins & Delisi (1990), as expected based on the rough core size: the wake descends by about 1.2 in a time of about 2. However, for times larger than they covered, we find dramatically different behaviour. The decrease in b, seen in figure 3, is delayed by about 1.5 units of Nt, but then occurs at about the same rate. By time $t = 4$, the vortices have reduced their spacing b by 75% and their circulation only by about 20%, and they break out of the initial bubble of light fluid. This is shown in figure 7, which is consistent with figures 2(f) and 3(f) in Robins & Delisi (1990) but with more structure as a result of the lower diffusion. The instantaneous stratification number is now much lower: $N^* \approx 0.06$. The spacing reduction is clearly initiated in figure 2 of Robins & Delisi (1990), but they do not comment and view the primary vortices as 'a residual vortex pair'. At later times b becomes as low as 0.03; the circulation then drops rapidly as a result of the cores touching. Around $t = 9$ the location of the vorticity peak jumps back to the region of activity left behind by the vortex pair, pointed out by Robins & Delisi (1990). While this jump is distracting (as well as Reynolds-number dependent), it usefully illustrates the large extent of the disturbed region. In any case, the head region has remained very active.

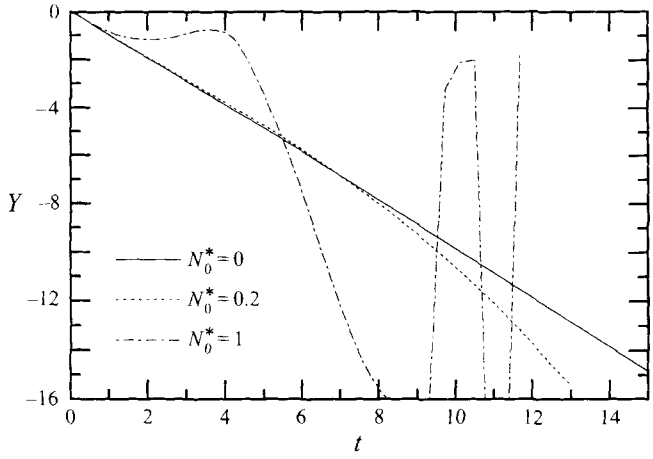

FIGURE 6. Propagation of Type-II wakes. $Re = 10^5$, $r_c = 0.01$.

With $N_0^* = 0.2$, the wake smoothly accelerates after a slight deceleration, and for the times of interest behaves like a Type-I wake. In particular, at $Nt = 2$, $b = 0.55$ which is close to figure 3. The cores do not touch, yet, and there is no circulation loss (Γ_1 was calculated). In summary, for representative clean-wing flows (and not just for tight vortices) the SD model is globally the correct one; it just does not apply as long as N^* is of the order of 1. The assertion that the descent is arrested around $Nt = \pi/2$ by stratification alone is simply incorrect.

It is unfortunate that the descent pattern seen in figure 6 is not amenable to a simple analytical description. In practical situations, neglecting the stratification effect would be a fair approximation for rather weak stratification (say $N_0^* \leqslant 0.5$). However for a very large airplane in strong stratification, leading to $N_0^* = 1$, it would not be correct, from an ATC point of view, to neglect the rise around time $t = 3$. Therefore, a measurement of the Brunt–Väisälä frequency and a comprehensive model of the stratification effect will both be needed if an optimum ATC strategy is to be devised.

4.4. *Type-III solutions*

As mentioned above the roll-up of Type-III solutions produces twin co-rotating vortices on each side. This is shown in figure 8(*a*). With $Re = 10^5$, $r_c = 0.01$, they persist until the time $t \approx 8$, barely sufficient to discern the interaction with stratification when $N_0^* = 0.2$. Figure 8(*b*) shows the density, which is passive since $N_0^* = 0$ but illustrates the shedding of light fluid by the tumbling vortices. Light fluid, as well as exhaust or other markers, is distributed along a 'curtain' over the primary vortices. Compare with figure 2(*b*, *d*). The shedding reduces the buoyancy effect (the area of light fluid is smaller than Cb^2, or if mixed, the average density anomaly is smaller than Y/L). Figure 9 shows the descent for $N_0^* = 0$, 0.2, and 1. The outboard vortex is stronger, and therefore the one detected by the search for an absolute vorticity maximum; it is the upper one in figure 8(*a*).

We first compare the $N_0^* = 0.2$ and $N_0^* = 0$ cases. Figure 9 displays the waviness characteristic of the tumbling twin-vortex system. As long as that system is in place, the descent is hardly affected by stratification. After that, a quasi-steady pattern is established and the stratified case accelerates, much like Types I and II. The delay, relative to Type II (figure 6), is only about 2 time units. We conjecture that at even higher Reynolds numbers merging does not occur within the time of interest; the

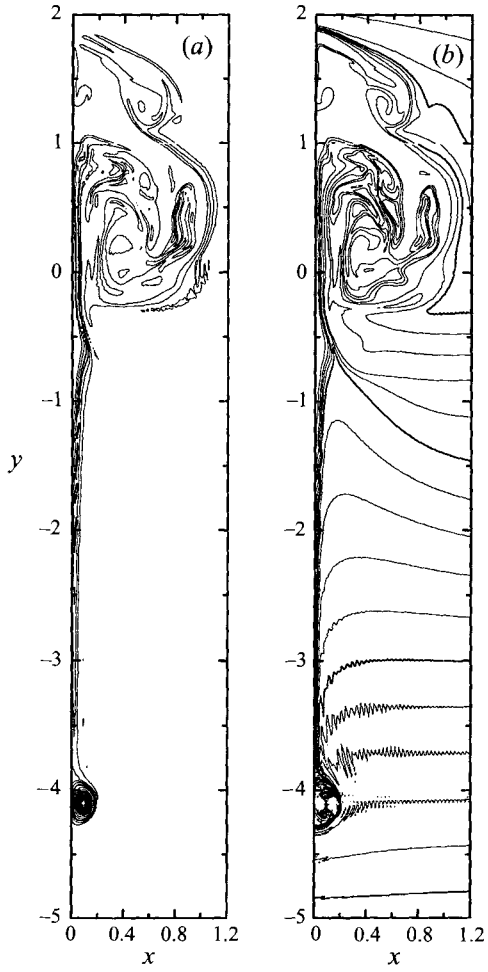

FIGURE 7. Distributions of (*a*) vorticity and (*b*) density in a solution of Type II, with $N_0^* = 1$.

result would be that the effect of weak stratification is largely suppressed by the twin-vortex structure. For now we can only report a modest effect; lift distributions that exaggerate that effect can of course be designed, but we believe our Type III to be typical of existing airplanes.

As before, the strongly stratified $N_0^* = 1$ case experiences a much slower descent at first. The waviness also disappears faster as a result of the buoyancy-generated vorticity mingling with the initial vorticity. Once merging has occurred, again the wake breaks out of the buoyant bubble and accelerates. We note that at $t = 4$ (a distance of the order of a nautical mile, for a very large airplane), it has returned almost to the initial level. The initial rebound is very strong (calculations at $N_0^* = 1.2$ show wakes returning all the way to the initial altitude). In this instance our result shows the wake closer to the flight path than even the simple models of 'finite descent and decay' would predict; the wake is also much more active than they would predict. We have not found any intuitive argument why Type-III wakes would return closer to the initial altitude; note that the acceleration around $t = 6$ is just as vigorous as for the other types, therefore it is not a case of energy depletion.

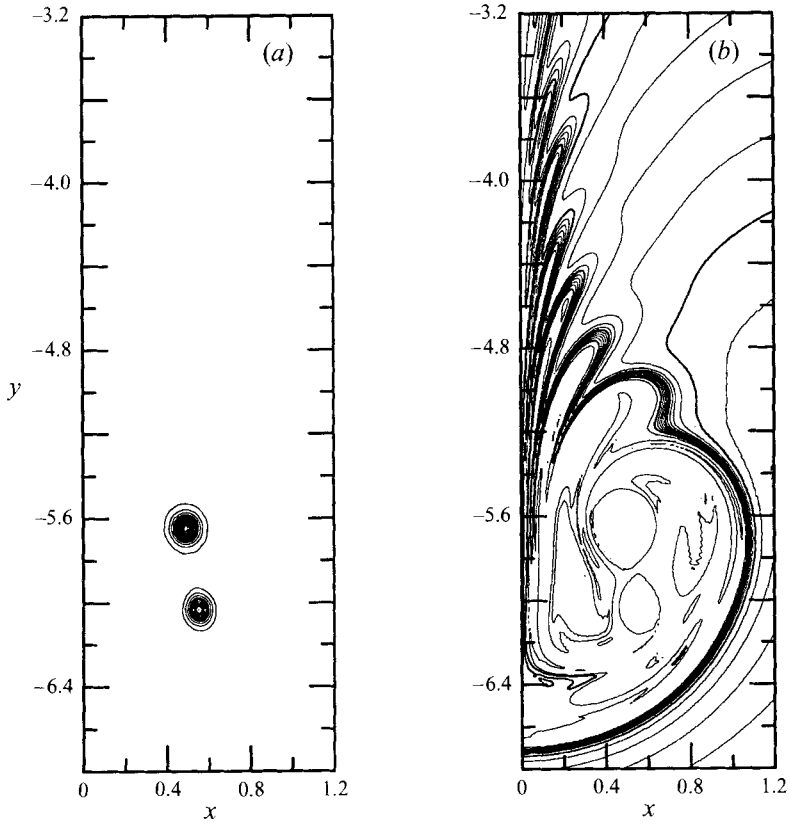

FIGURE 8. Distributions of (*a*) vorticity and (*b*) density in Type-III flow, $N_0^* = 0$, $Re = 10^5$, $r_c = 0.01$, $t = 6$.

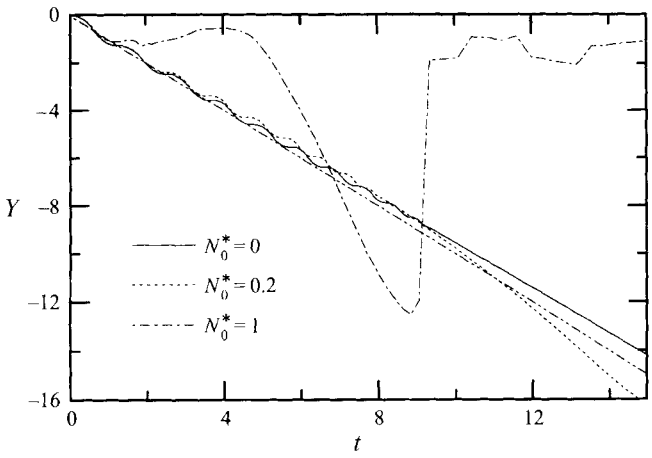

FIGURE 9. Propagation of Type-III wakes in a stratified fluid. $Re = 10^5$, $r_c = 0.01$. - - — - -, $Y = -t$.

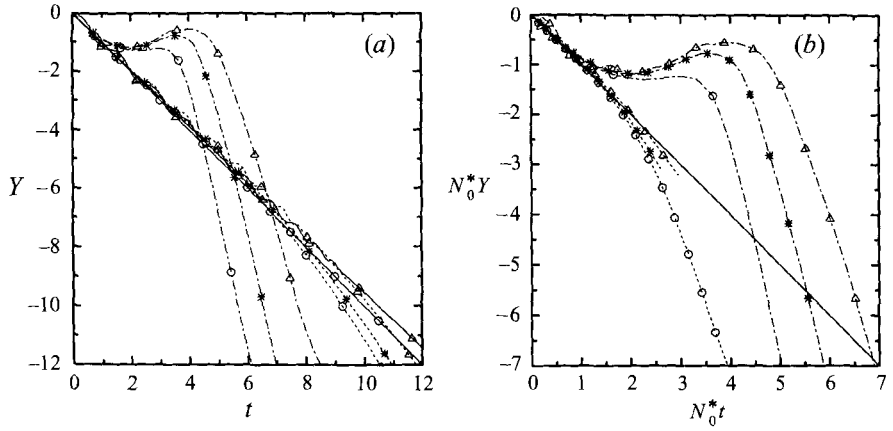

FIGURE 10. Propagation of wakes in a stratified fluid. (*a*) *vs.* t; (*b*) *vs.* N_0^*t. ○, Type I; *, Type II; △, Type III. —, $N_0^* = 0$; - - -, $N_0^* = 0.2$; - — -, $N_0^* = 1$.

5. Discussion

5.1. *Overall predictive capabilities*

We believe that the controversy described by Widnall (1975) is solved, in the 2DLD clean-wing setting. We have provided very supportive numerical results, including realistic vortex core sizes, and a clarification that makes the SD formulas (9) more convincing. In air-traffic practice, the level of stratification can exceed the range of validity of these formulas, and we obtained somewhat surprising numerical results. Figure 10 presents the propagation of all the wakes considered above: Types I, II, and III; initial stratification numbers $N_0^* = 0$, 0.2, and 1. The results are shown versus 'wake time' t and versus 'Brunt–Väisälä time' N_0^*t, in a search for a normalization that collapses many cases. The rebound with $N_0^* = 1$ is weaker for Type I than for II and III. Globally, the curves do not collapse, and do not even have shapes similar enough to suggest that a normalisation exists that would achieve a useful collapse. In particular the SD formulas (9) capture the evolution only when the instantaneous stratification number N^* is at most equal to about 1/4, meaning a moderately weak stratification, and then with a time shift that is very meaningful in practice. We note that when N_0^*Y is relatively large (say of the order of −6) all the curves have about the same slope in figure 10(*b*), which is consistent with (9*a*) provided we allow for a virtual origin in time. Although the propagation of the vorticity peak does not represent all the information of interest, the fact that its behaviour seems out of reach of a simple formula indicates that a description of the physics by just a few empirical equations will not be devised easily.

We experimented with an extended system of ordinary differential equations (ODEs), compared with (6)–(8). The effect of ω_2 on the descent velocity was not neglected, and we replaced (7) with $\mathrm{d}Y/\mathrm{d}t = -(\Gamma_0 + C_3\Gamma_2)/(2\pi b)$ (equivalent to (4.6*b*) in Crow (1974)) where C_1C_3 appears to be between 20 and 30 according to our Type-I, $N_0^* \leqslant 0.2$ solutions. This provided little improvement for the $N_0^* = 1$ case, very probably because (6) is not established rapidly enough. Upgrading (6) seems more difficult, as many effects compete during the initial roll-up that are hardly reducible to a few ODEs. Ultimately, ODEs that exploit only the circulation and the impulse cannot be expected to distinguish between the three flow types.

We also tested Crow's (1974) equation (9.6), a correction for "buoyant upwash". This correction is of order N_0^* and therefore larger than that in the preceding paragraph or in Crow's own (4.6*b*). In his notation, we plotted $\mathrm{d}h/\mathrm{d}t + 1/s$ versus $-\epsilon s^2 h/8\pi$, for $N_0^* = 0.2$ and 0.1. We were unable to identify a régime in which the two were clearly proportional (β would then be constant). Comparisons between his figure 12 and our figure 3 are also inconclusive. He predicts a smaller b for larger N_0^*. The $N_0^* t \leqslant 1$ region shows clear disagreement; it is possible that the flow evolves towards the region of validity of his theory later, as suggested by the steeper slope of our $N_0^* = 0.2$ curve for $N_0^* t \geqslant 1$. In any case, his figure 11 shows no sign of the rebound we wish to reproduce, therefore the difficulty with N_0^* of order 1 remains.

Our results invalidate the widespread idea that the wake descends for roughly 1/4 of the Brunt–Väisälä period ($N_0^* t = \pi/2$ in figure 10*b*) and then decays, at least in the 2DLD setting. Kinetic energy is, of course, lost to the buoyancy, but the vortex pair absorbs that loss by reducing its spacing (while roughly preserving its core size) and not by reducing its peak vorticity or velocity. The latter measures of the wake intensity are more significant than the kinetic energy in the case of interaction with another airplane. The reduction in spacing will precipitate the decay only once the vortex cores start touching, which happens during the duration of interest only for quite high stratification numbers, say $N_0^* \geqslant 1/2$.

The intuitive expectation that stable stratification impedes motion, and promotes oscillations, is not completely contradicted by our results. As explained by Robins & Delisi (1990), the kinetic energy is depleted, and both kinetic and potential energy can be considered as deposited on a kind of a curtain along the path of descent (their figures 5–6, our 7). The kinetic energy in the head of the wake *is* depleted. We also found that the total impulse of the flow oscillates in time, very close to the Brunt–Väisälä frequency (it contains a large contribution from the tail region). This could be attributed to an internal-wave phenomenon. Thus, depending on which aspect of the flow we consider, it can be viewed as diverging, damped, or oscillatory. The behaviour is more complex than has been thought.

We also note that the salient features of our results, namely the reduction in vortex spacing and the increase in descent velocity, can be tested by flow visualization. The apparent span indicated by dye in the vortex cores obeys (8). The experimental challenges are to reach a low enough level of mixing, viscous or turbulent, to obtain a reasonable segregation between the two vorticity patches, and more crucially to delay the Crow instability. The value $N_0^* = 0.2$ would be useful, as the spacing reduction is a measurable 20% after a descent equal to 6 times the initial spacing. Such descents have been obtained in laboratories, but unfortunately not for stratified flow (Sarpkaya 1983). Larger values such as $N_0^* = 1$ are not desirable because the spacing reduction is fortuitously delayed until $t > 3$, both in our simulations (not shown) and in experiments (NorthWest Research Associates, private communication 1996).

5.2. *Destruction mechanisms*

Many mechanisms for instability and mixing are available in real flows, and not in our two-dimensional study. Therefore, separate estimates are desirable; we review candidate mechanisms in turn. As explained in §1.2 we are doubtful of turbulent mixing internal to the primary vortices, and will not discuss it further. Molecular mixing is negligible at flight Reynolds numbers, of course.

In weakly stratified cases such as in figure 2, we have not seen Kelvin–Helmholtz corrugations on the ω_2 sheet (unlike on ω_1 during roll-up). We presume that ω_2 is

too weak for sizeable growth to occur (the fluid carrying ω_2 is rapidly detrained). The more strongly stratified cases generate much more convoluted structures (Robins & Delisi 1990, figure 3, our figures 7 and 8) and the attendant steep gradients cause more dissipation. However, in most cases the wake succeeds in reducing N to the order of 0.2 and less, leading to situations closer to figure 2 after a few time units. The ω_2 layer could also support three-dimensional turbulence, as its curvature is conducive to a centrifugal instability. This is out of reach of the present code, but we observe that the associated mixing rate would very likely again scale with Γ_2, which is much smaller than Γ_1. In principle, this mixing was captured by the turbulence model of Hecht *et al.* (1981).

A decay mechanism that is accessible to our method, and probably beginning for $t > 3$ in figure 3, is contact between the two cores accompanied by detrainment of primary vorticity (ω_1). For Type-II cases, which have a non-arbitrary core size, we see from figure 5 that definite contact will occur when b has dropped by 40%, which figure 3(b) shows to be well within the range of interest. Another view is that the kinetic energy of the vortex pair is proportional to $\log(b/r_e)$ with r_e an effective core radius. According to (9), b decreases exponentially whereas r_e cannot decrease, therefore the kinetic energy of the pair decreases linearly. This must cease at finite time, since in Type II the initial energy is finite (about 0.4, based on Γ_0). In a simple method an energy argument would probably be helpful to estimate decay by contact but, again, it would be accurate only for weak stratification.

SD propose the following destruction mechanism for the stratified wake. The detrainment of ω_2 shown in figure 2(c) is dependent on the field $\boldsymbol{U}_2$ itself creating a clearance between the ω_2 layer and the upper stagnation point, and as Γ_2 decreases to 0 full detrainment cannot occur any more. As soon as ω_2 is partly entrained, a situation with closed streamlines and circulation decreasing outward is created, and rapidly 'leads to a breakdown of the vortices'. SD must envision a curvature-driven instability, therefore three-dimensional and out of reach of our method. However, entrainment should cause an increase in $|\Gamma_2|$; we have not seen this within the duration of our simulations. We also note that an instability affecting a much-weakened ω_2 field (in figure 2c, Γ_2 is only -0.013) may not have much leverage over the primary vortices, especially if the circulation distribution of those gradually rises with radius as in figure 5, which is stabilizing (SD envisioned only point or tight vortices). We await evidence that this decay mechanism is effective.

A very convincing proposal is the enhancement of the Crow instability (Crow 1970) by the decrease in effective span. The Crow growth rates scale with b^{-2}, and therefore can increase many times in some cases. Since the instability is not very selective of wavelengths and has a unique mode shape, very favourable growth ratios can be expected. We do not expect stratification to influence the growth rates directly, as the density gradients occur away from the primary vortices, and use Crow's unstratified results for the rates. Consider Sarpkaya's (1983) figure 13, for rounded tips, cases $N_0^* = 0$ and 0.5. The maximum travel is $6.1b_0$ and $4.7b_0$, respectively. With $N_0^* = 0$ and the classical wavelength $\lambda = 8.6b_0$, the Crow amplitude ratio at the time for $Y = -6.1$ is 155. With $N_0^* = 0.5$ and a wavelength $\lambda = 5b_0$, the Crow amplitude ratio at the time for $Y = -4.7$ is about 135 (based on approximately integrating $1/b^2$ from figure 3 times Crow's growth rates for different β). We further observe that b has been roughly halved, which halves the amplitude needed for the vortices to make contact and initiate 'pinching'. On the other hand if, like Crow, we assume a Kolmogorov spectrum, the turbulent velocity scale at $5b_0$ is only 0.84 times that at $8.6b_0$. That leads to an 'effective' growth ratio of 230 for $N_0^* = 0.5$. This number is close enough to 155

to make this mechanism quite consistent with Sarpkaya's results (we motivate the words 'close enough' by the fact that $\log(230)/\log(155) = 1.08$ whereas $4.7/6.1 = 0.77$). The uncertainty in the 'receptivity' coefficient and in the actual slope of the turbulence spectrum easily account for a factor of 155/230. We also neglected the possibility that the stratified tank had a lower turbulence level, which would bring the number down from 230. We concede that Sarpkaya did not find support for a decrease of b, but he clearly concluded that stratification arrests the descent only in "collaboration" with other mechanisms. In recent three-dimensional simulations, Robins & Delisi (1995) are indeed finding that stratification promotes the Crow instability and linking. We expect that further simulations of this type (preferably with natural stimulation of the instability) and further experiments (preferably with better control of the external disturbances), will narrow the gap between 2DLD results and laboratory tests. Combined, they will build our understanding of the full-size wakes.

We benefited from numerous discussions with Mr Robins of NorthWest Research Associates, Dr Coleman of UCLA, and Drs Bays-Muchmore and Crouch of Boeing. We thank all four referees for substantial comments. The mainframe computer time was donated by NAS.

REFERENCES

Bruin, A. C. de, Hegen, S. H., Rohne, P. B. & Spalart, P. R. 1996 Flow field survey in trailing vortex system behind a civil aircraft model at high lift. *AGARD Symp. on The Characterisation and Modification of Wakes from Lifting Vehicles in Fluids, Trondheim, Norway, 20–23 May.*

Charney, J. G. & Drazin, P. G 1961 Propagation of planetary-scale disturbances from the lower into the upper atmosphere. *J. Geophys. Res.* **66**, 83–109.

Crow, S. C. 1970 Stability theory for a pair of trailing vortices. *AIAA J.* **8**, 2172–2179.

Crow, S. C. 1974 Motion of a vortex pair in a stably stratified fluid. *Poseidon Research Rep.* No. 1. Santa Monica, CA.

Devenport, W. J., Rife, M. C., Liapis, S. A. & Follin, G. J. 1996 The structure and development of a wing-tip vortex *J. Fluid Mech.* **312**, 67–106.

Gottlieb, D. & Orszag, S. A. 1977 *Numerical Analysis of Spectral Methods.* SIAM, Philadelphia.

Govindaraju, S. P. & Saffman, P. G. 1971 Flow in a turbulent trailing vortex. *Phys. Fluids* **14, 10**, 2074–2080.

Greene, G. C. 1986 An approximate model of vortex decay in the atmosphere. *J. Aircraft* **23, 7**, 566–573.

Hecht, A. M., Bilanin, A. J. & Hirsh, J. E. 1981 Turbulent trailing vortices in stratified fluids *AIAA J.* **19**, 691–698.

Hill, F. M. 1975 A numerical study of the descent of a vortex pair in a stably stratified atmosphere *J. Fluid Mech.* **71**, 1–13.

Hoffmann, E. R. & Joubert P. N. 1963 Turbulent line vortices. *J. Fluid Mech.* **16**, 395–411.

Lamb, H. 1932 *Hydrodynamics*, 6th edn. Dover.

Liu, H.-T. & Srnsky, R. A. 1990 Laboratory investigation of atmospheric effects on vortex wakes. *Tech. Rep.* 497. Flow Research, Inc., Kent, WA.

Milne-Thomson, L. M. 1958 *Theoretical Aerodynamics.* Dover.

Moore, D. W. & Saffman, P. G. 1973 Axial flow in laminar trailing vortices. *Proc. R. Soc. Lond.* A **333**, 491–508.

Phillips, W. R. C. & Graham, J. A. H. 1984 Reynolds stress measurements in a turbulent trailing vortex. *J. Fluid Mech.* **147**, 353–371.

Robins, R. E. & Delisi, D. P. 1990 Numerical study of vertical shear and stratification effects on the evolution of a vortex pair. *AIAA J.* **28**, 661–669.

Robins, R. E. & Delisi, D. P. 1995 3-D Calculations showing the effects of stratification on the evolution of trailing vortices. *Proc. IMACS-COST Conf. on Comp. Fluid Dyn.: Three-Dimensional Complex Flows. Sept. 13–15, 1995, Ecole Polytechnique Fédérale de Lausanne, Switzerland.*

SAFFMAN, P. G. 1972 The motion of a vortex pair in a stratified atmosphere. *SIAM* **LI, 2**, 107–119.

SARPKAYA, T. 1983 Trailing vortices in homogeneous and density-stratified media. *J. Fluid Mech.* **136**, 85–109.

SCORER, R. S. & DAVENPORT, L. J. 1970 Contrails and aircraft downwash. *J. Fluid Mech.* **43**, 451–464 (referred to herein as SD).

SPALART, P. R., MOSER, R. D. & ROGERS, M. M. 1991 Spectral solvers for the Navier-Stokes equations with two periodic and one infinite direction. *J. Comput. Phys.* **96, 2**, 297–324.

SPREITER, J. R. & SACKS, A. H. 1951 The rolling up of the trailing vortex sheet and its effect on the downwash behind wings. *J. Aero. Sci.* **18**, 21–32.

TOMASSIAN, J. D. 1979 The motion of a vortex pair in a stratified medium. Doctoral Dissertation, University California, Los Angeles.

TURNER, J. S. 1960 A comparison between buoyant vortex rings and vortex pairs. *J. Fluid Mech.* **7**, 419–433.

WIDNALL, S. E. 1975 The structure and dynamics of vortex filaments. *Ann. Rev. Fluid Mech.* **7**, 141–165.

ZEMAN, O. 1995 The persistence of trailing vortices: a modeling study. *Phys. Fluids* A **7**, 135–143.